Electronic Supplementary Information

Carbon Dots with Induced Surface Oxidation Permits Imaging at Single-Particle Level for Intracellular Studies

Santosh K. Misra,[‡,a] Indrajit Srivastava,[‡,a] John S. Khamo,[b] Vishnu V. Krishnamurthy,[b] Dinabandhu Sar, [a] Aaron S. Schwartz-Duval,[a] Julio A. N. T. Soares,[6] Kai Zhang, [b'd *] and Dipanjan Pan [a,*]

[a]Department of Bioengineering, Beckman Institute, Department of Materials Science and Engineering, University of Illinois at Urbana-Champaign, Illinois, USA

Carle Foundation Hospital, 611 West Park Street, Urbana, IL, USA

[b]Department of Biochemistry, University of Illinois at Urbana-Champaign, Urbana, Illinois 61801, USA

[c]Frederick Seitz Materials Research Laboratory Central research facilities, University of Illinois at Urbana-Champaign, Urbana, Illinois, USA.

[d]Neuroscience Program, University of Illinois at Urbana-Champaign, Urbana, Illinois 61801, USA

Center for Biophysics and Quantitative Biology, University of Illinois at Urbana-Champaign, Urbana, Illinois, USA.

‡Authors contributed equally to this work.

*To whom correspondence should be addressed: E-mail: kaizkaiz@illinois.edu and dipanjan@illinois.edu

S.N.	Content	Page No.
1.	Hydrodynamic diameter measurement and Zeta potential of CD 24h	S3
2.	Hydrodynamic diameter measurements of CD-NMMO after 1 h, 2 h and 8 h	S4
3.	Hydrodynamic diameter measurement of CD-NMMO after 24 h	S5
4.	Changes in UV-Vis absorption profiles of CD-NMMO after 1 h, 2 h, 8 h and 24 h	S6
5.	Changes in ζ-potential of CD-NMMO with an increase in hydrothermal treatment	S7
6.	Fourier Transform-Infra Red (FT-IR) spectroscopic features of CDs	S8
7.	Raman spectroscopic features of CD-NMMO 24 h, and CD 24 h	S9
8.	Fluorescence emission spectra of CD-NMMO 24 h, and CD 24 h	S10
9.	Chromatographic separation of CD-NMMO particles in four fractions of CDs	S11
10.	IVIS study on CDs and CD-NMMOs	S12
11.	Intracellular image analysis of C32 cells incubated with CD-NMMO	S13
12.	Intracellular image analysis of C32 cells incubated with different fractions	S14
13.	Mass spectra of CD-NMMO 24 h	S15
14.	Mass spectra of CD-NMMO 1 h	S16
15.	Mass spectra of CD-NMMO 2 h	S17
16.	Mass spectra of CD-NMMO 8 h	S18
17.	Time-resolved photoluminescence value of CD-NMMO and CD-NMMO fractions	S19
18.	Quantum yield table	S20

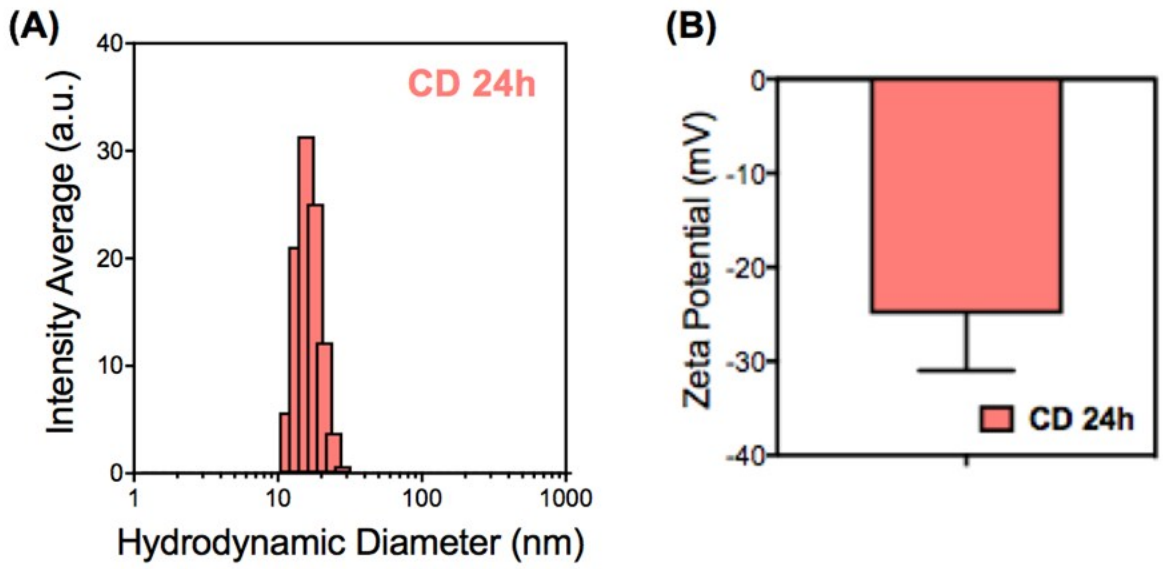

Figure S1. (A) Hydrodynamic diameter measurements of CD after 24h of hydrothermal treatment; (B) Corresponding zeta potential measurement of CD 24h demonstrating a negative potential.

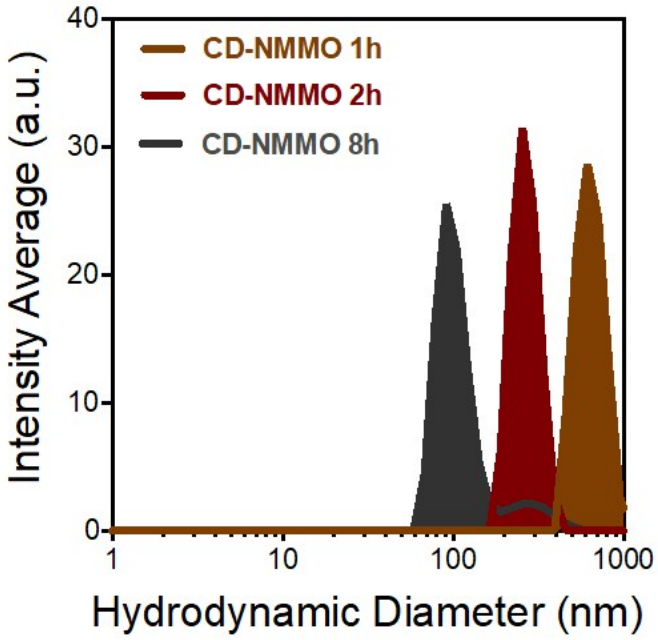

Figure S2. Hydrodynamic diameter measurements of CD-NMMO after 1 h, 2 h and 8 h of hydrothermal treatment.

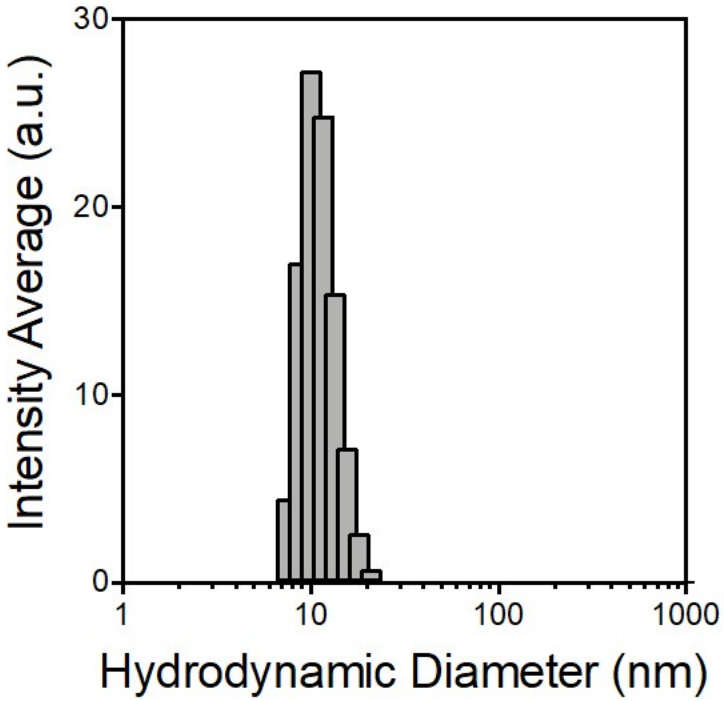

Figure S3. Hydrodynamic diameter measurement of CD-NMMO after 24 h hydrothermal synthesis.

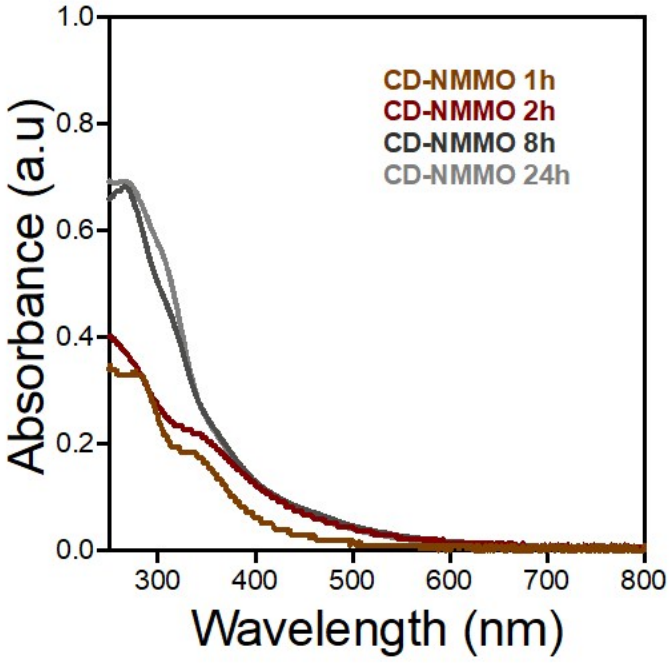

Figure S4. Changes in UV-Vis absorption profiles of CD-NMMO after 1 h, 2 h, 8 h and 24 h of hydrothermal treatment.

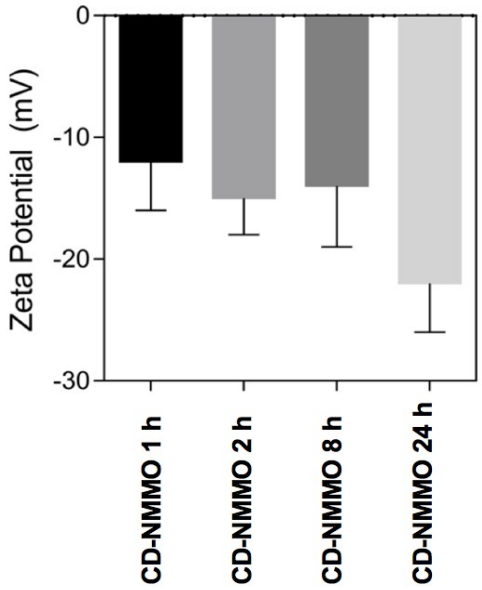

Figure S5. Changes in ζ-potential of CD-NMMO with an increase in hydrothermal treatment time.

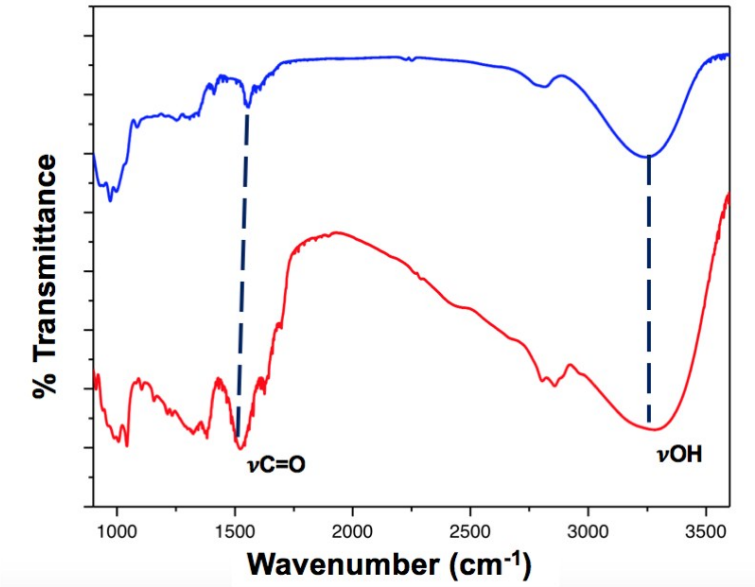

Figure S6. Fourier Transform-Infra Red (FT-IR) spectroscopic features of CD 24 h (blue) and CD-NMMO 24 h (red).

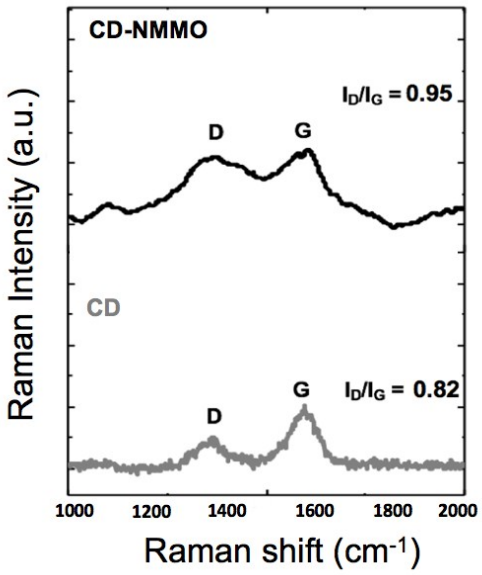

Figure S7. Raman spectroscopic features of CD-NMMO 24 h, and CD 24 h (Top/Bottom), respectively. Characteristic D and G bands from carbon nanoparticles feature in both the samples.

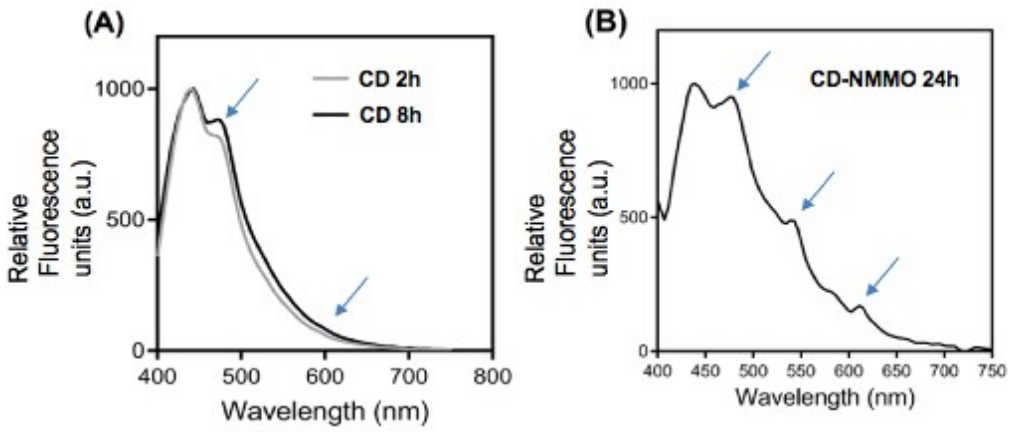

Figure S8. (A) Fluorescence emission of CDs synthesized by hydrothermal treatment of sucrose for 24h (CD 24 h), respectively, excited at 360 nm. (B) Fluorescence emission of CD-NMMO synthesized by hydrothermal treatment of sucrose and NMMO for 24h (CD-NMMO 24 h), excited at 360 nm.

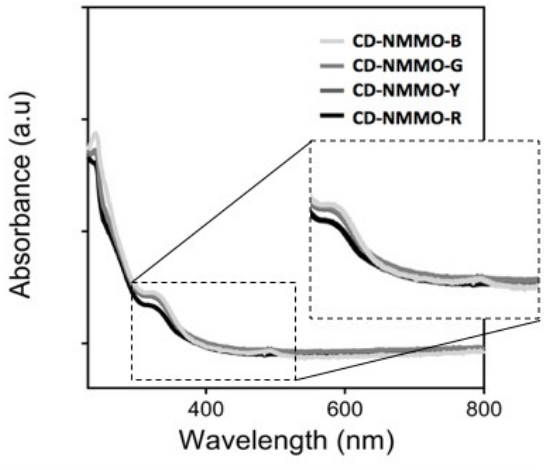

Figure S9. Chromatographic column separation of CD-NMMO particles in four fractions of CDs with different physicochemical and respective optical properties. Absorption efficiency for different fractions ranging from blue, green, yellow to red.

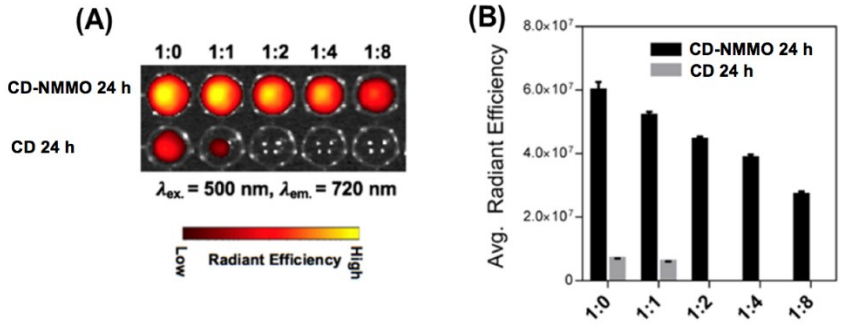

Figure S10. (A) Fluorescence imaging signals of CD-NMMO and CD *via* IVIS under excitation at 520 nm and getting the emission at 720 nm. (B) Corresponding radiant efficiency values were compared at each dilution.

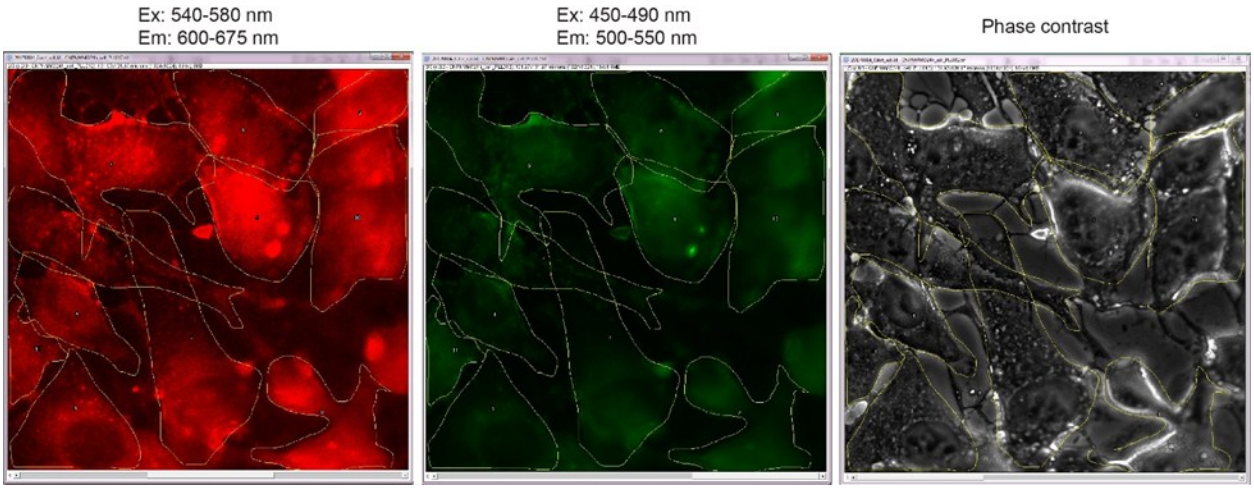

Figure S11. Single-cell image analysis of C32 cells incubated with CD-NMMO. For each field of view, three channels (Red, Green, Phase Contrast) were used to capture cell image. The region of interest *(ROI) Manager* plugin from FIJI was used to analyse the correlation of fluorescence intensities for each channel.

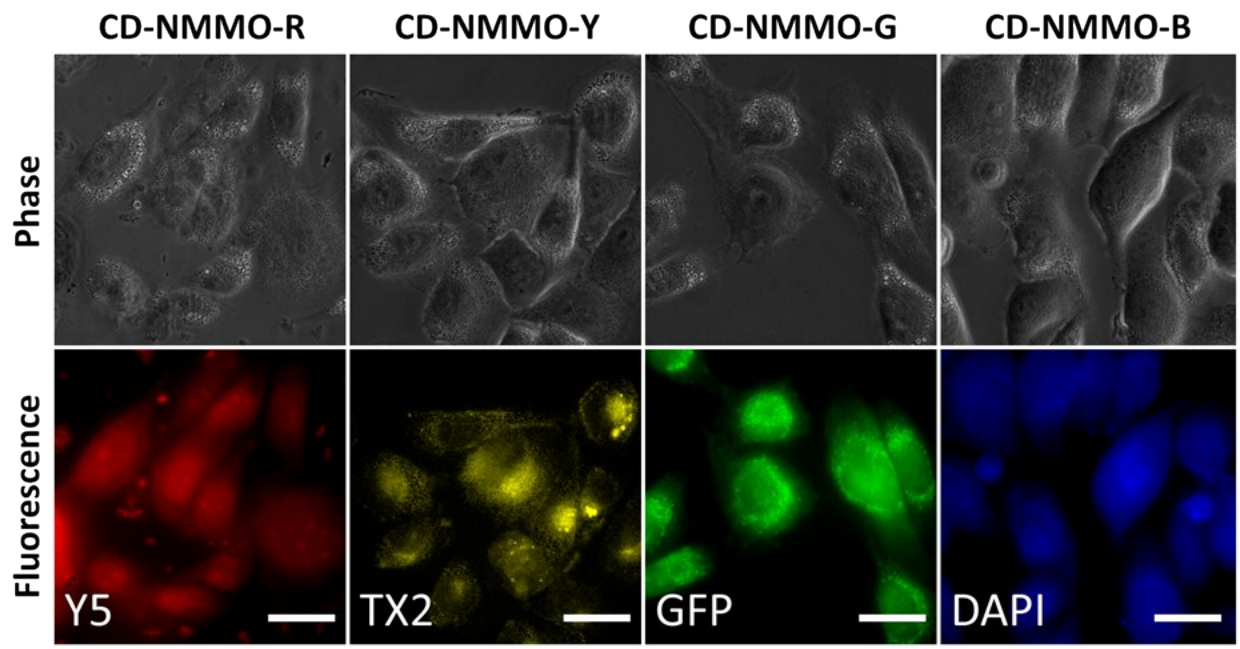

Figure S12. Intracellular image analysis of C32 cells incubated with different fractions of CD-NMMO including CD-NMMO-B, CD-NMMO-G, CD-NMMO-Y, and CD-NMMO-R acquired under DAPI, GFP, TX2 and Y5 regions, respectively. For each field of view, two channels (Color and Phase Contrast) were used to capture cell image. The region of interest (ROI) Manager plugin from FIJI was used to analyze the correlation of fluorescence intensities for each channel. Scale bar is 30 μm.

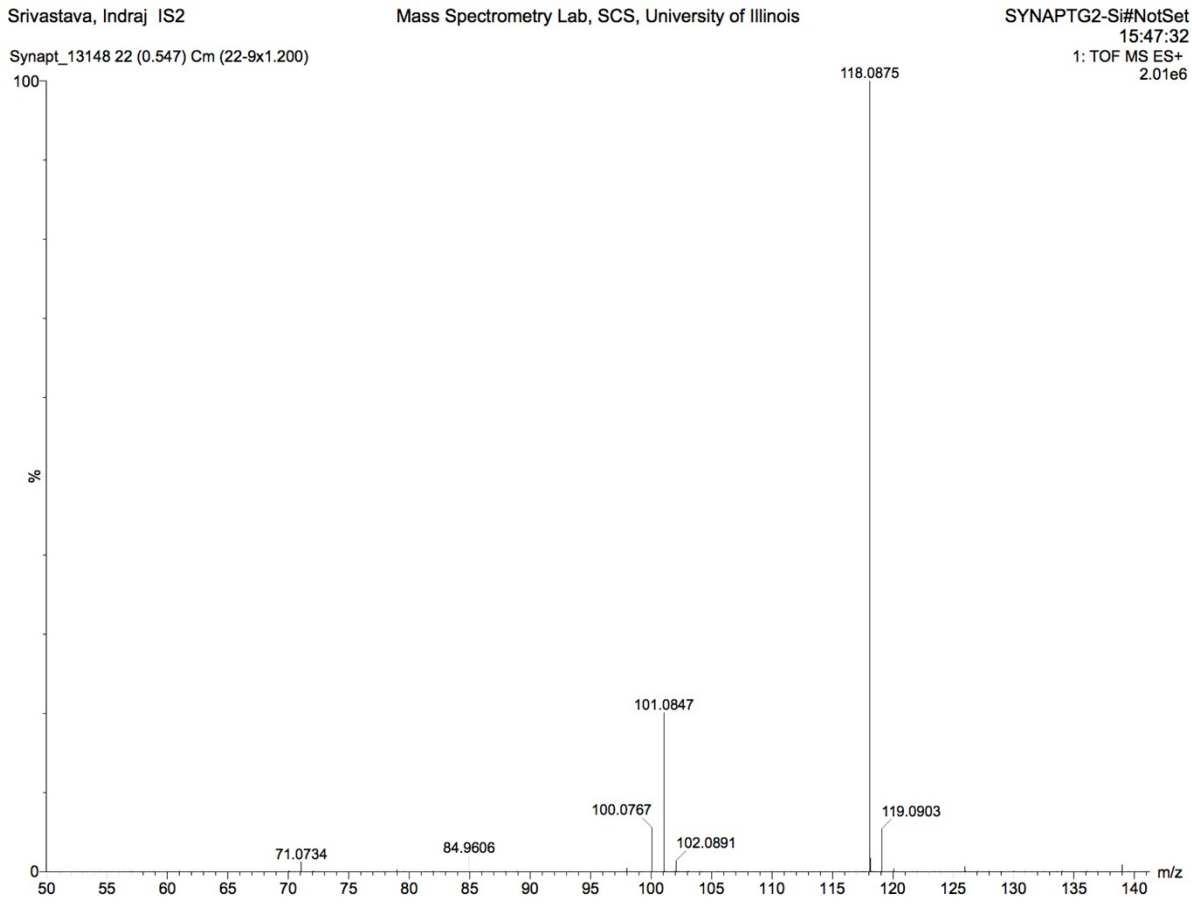

Spectra S1. Molecular ion peak of NMMO (118.0875) in mass spectrum obtained by hydrothermal treatment of NMMO for 24 h.

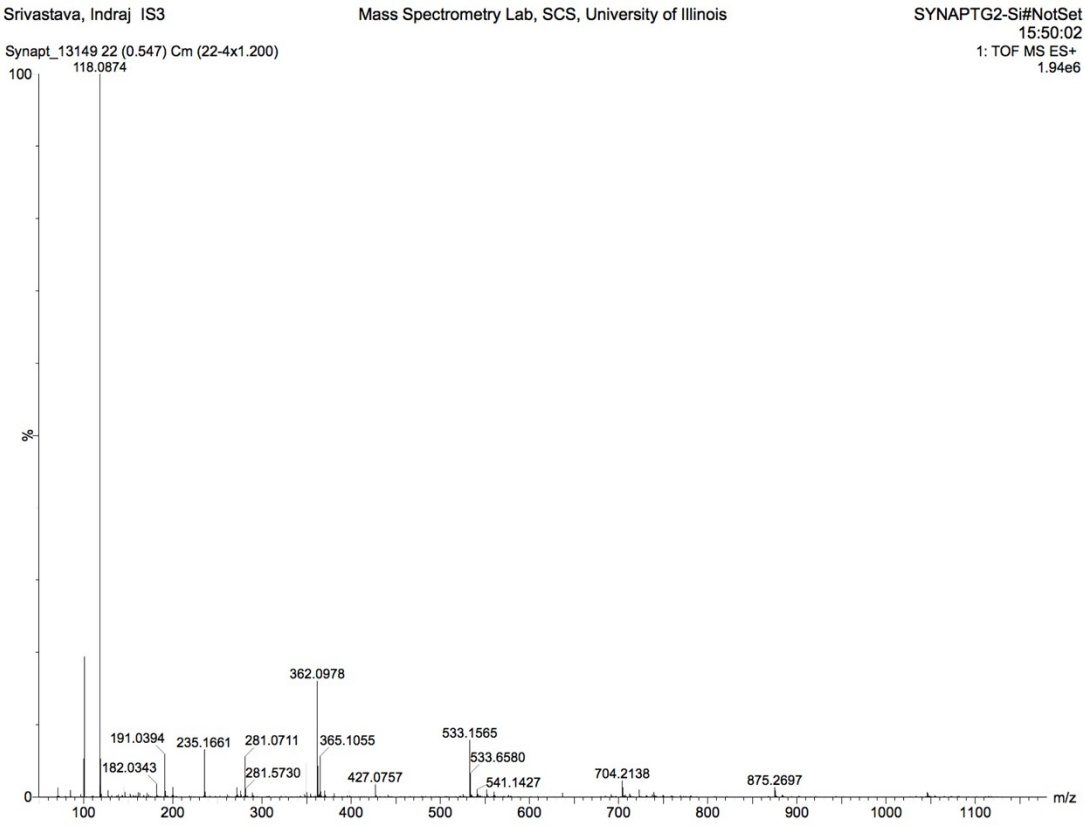

Spectra S2. Molecular ion peak of NMMO (118.0875) in mass spectrum obtained by hydrothermal treatment of CD-NMMO for 1 h.

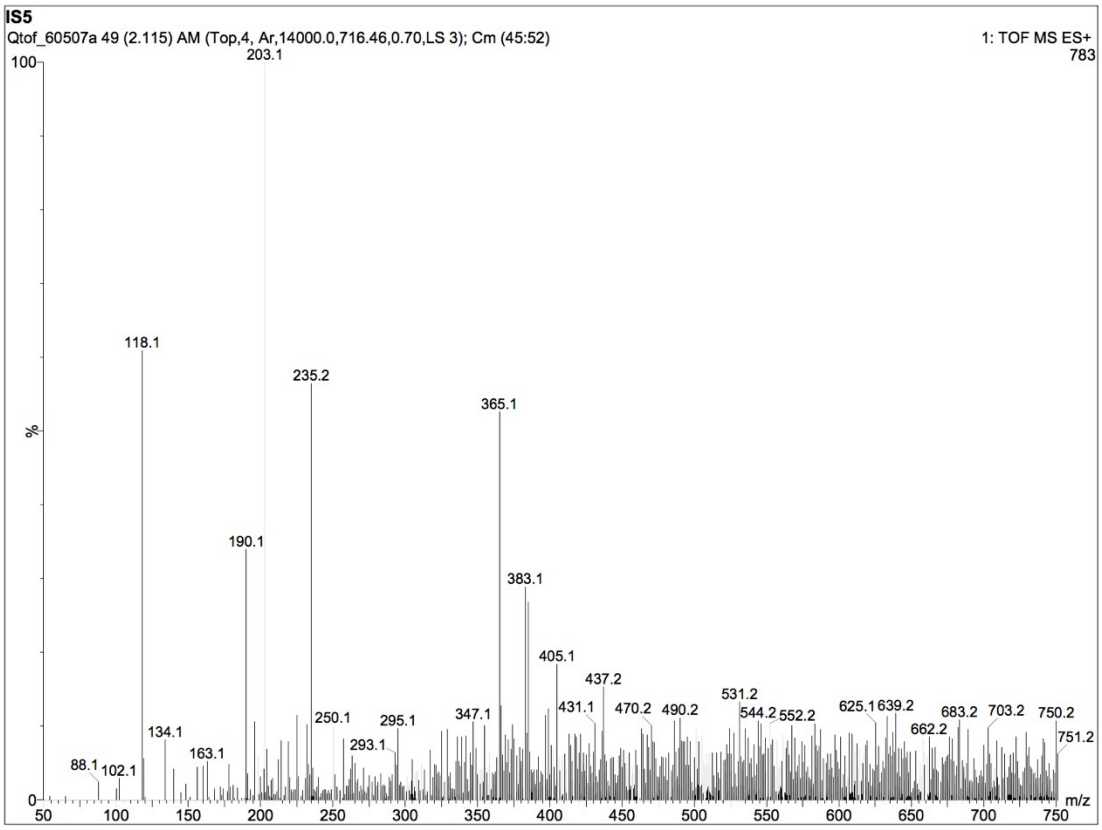

Spectra S3. Molecular ion peak of NMMO (118.0875) in mass spectrum obtained by hydrothermal treatment of CD-NMMO for 2 h.

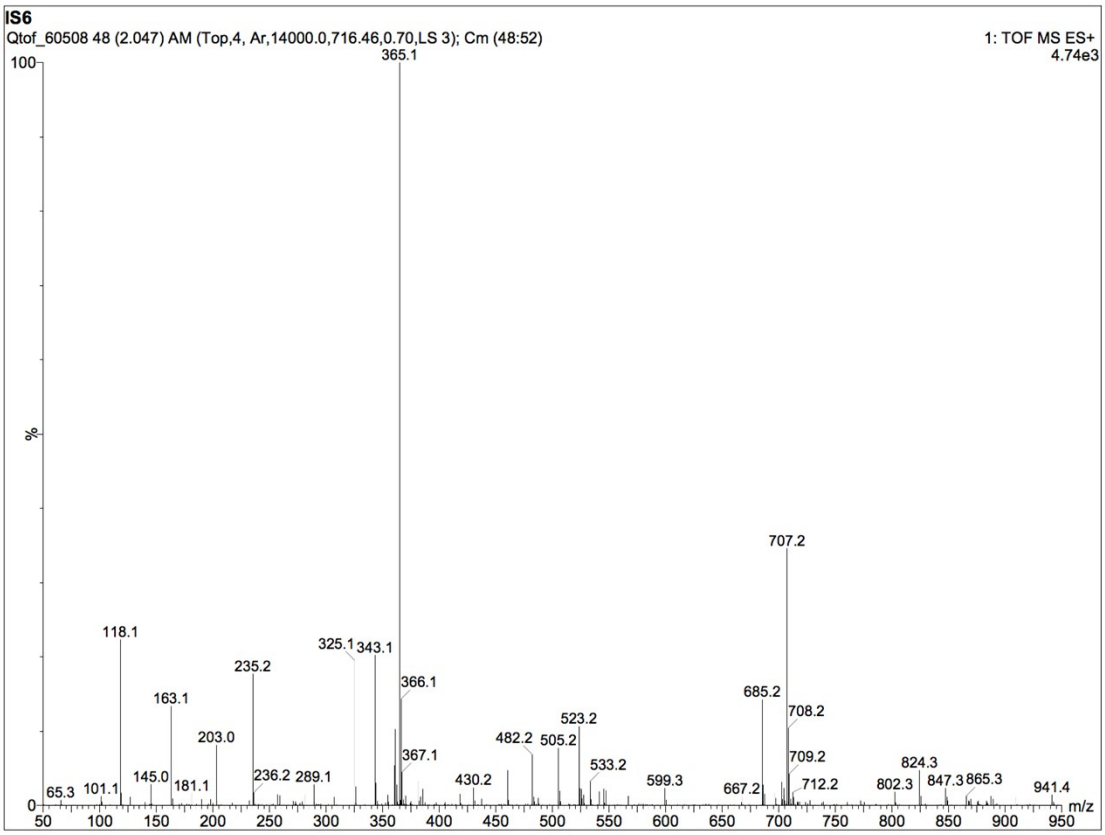

Spectra S4. Molecular ion peak of NMMO (118.0875) in mass spectrum obtained by hydrothermal treatment of CD-NMMO for 8 h.

Table S1 Time-resolved photoluminescence value of CD-NMMO and CD-NMMO fractions obtained *via* column chromatography excited at different wavelengths

Samples	Excitation Wavelength (nm)	$t_{1/2}$	Chi-square
CD-NMMO	390	3.072	13.1
CD-NMMO-B	390	2.718	6.92
CD-NMMO-G	390	2.689	1.74
CD-NMMO-Y	390	3.101	7.68
CD-NMMO-R	390	3.176	4.87
CD-NMMO-R	510	5.457	11.8

Table S2. Quantum yields of CD fractions using quinine sulfate as reference.

Samples	Integrated Emission Intensity (I)	Refractive Index of solvent (µ)	Quantum yield (Ø)
Quinine sulfate	601322	1.33	0.54
CD	65934.4	1.33	0.16
CD-NMMO-B	99399.8	1.33	0.21
CD-NMMO-G	186585	1.33	0.26
FITC	354769.8	1.75	0.95
CD-NMMO-Y	202412.86	1.33	0.236
CD-NMMO-G	233478.19	1.33	0.244